Reference: *Biol. Bull.* **174:** 67–76. (February, 1988)

A Physiological Comparison of Bivalve Mollusc Cerebro-visceral Connectives With and Without Neurohemoglobin. II. Neurohemoglobin Characteristics

JEANNETTE E. DOELLER[a] AND DAVID W. KRAUS[a,b]

Department of Biological Sciences, Clemson University, Clemson, South Carolina 29634-1903

Abstract. Several bivalve mollusc species possess hemoglobin in their nervous systems whereas most species do not. The function of this neurohemoglobin was investigated *in situ* in cerebro-visceral connectives of *Tellina alternata* and *Spisula solidissima*. Both neurohemoglobins, located in glial cells, exhibit high oxygen affinities and relatively high Hill numbers. The rate of oxygen diffusion into the connective begins to fall below the consumption rate near the PO_2 at which each neurohemoglobin begins to unload oxygen, assuming the perineural sheath presents an effective barrier to oxygen diffusion. The neurohemoglobin could thus act as an oxygen store during periods of low PO_2.

Oxygen unloading from the neurohemoglobin proceeds for a considerable length of time at a constant rate. The long duration may be attributed to the geometry of the connective and to the perineural sheath, whose primary function may be to retain oxygen within the connective during anoxic conditions. The constant unloading rate may be attributed to neurohemoglobin cooperativity *in situ* because the driving force for unloading remains nearly constant at the P_{50} of each neurohemoglobin. An oxygen supply at a constant rate for an extended period of time would be useful to an animal requiring aerobic nervous function during anoxic conditions.

Introduction

A substantial amount of hemoglobin can be present in a particular tissue of one or a few species and absent in the homologous tissue of other related species. Such uncommon occurrences of hemoglobin may be supported by other adaptations (biochemical, physiological, morphological, and/or behavioral) that have secured its production. For example, only a few species of the many aquatic true bugs (Hemiptera) possess hemoglobin and it may be used for precise buoyancy regulation when the organism is submerged (Wells *et al.*, 1981). Likewise, only a small number of the multitude of meiofaunal species possess hemoglobin (Kraus and Colacino, 1984). The slowly unloading hemoglobin in *Neodasys* spp. (Gastrotricha) may provide a scuba tank of oxygen for use during excursions into anoxic zones (Colacino and Kraus, 1984). Only a few species of brittlestars (Ophiuroidae) circulate hemoglobin in their water-vascular system, possibly compensating for the lack of respiratory and reproductive bursae (Heatwole, 1981). In contrast, the terebellids (Polychaetae) possess circulating hemoglobin as a general rule, but *Lysilla alba*, which is sympatric with sanguineous species, is devoid of hemoglobin. It may compensate by more vigorous burrow ventilation (Mangum *et al.*, 1975). These examples suggest that the specific services of hemoglobin may be as diverse as the organisms themselves.

Hemoglobin is found in the nervous systems of only a few species of bivalve molluscs (Kraus *et al.*, 1988). Mollusc neurohemoglobins have been previously studied with regard to spectral and molecular properties (Strittmatter and Burch, 1963; Wittenberg *et al.*, 1965) and functional characteristics (Kennedy, 1960; Chalonzonitis *et al.*, 1965; Kraus and Colacino, 1986). Kennedy (1960) argued that hemoglobin in the nerves of *Spisula*

Received 22 June 1987; accepted 30 November 1987.

[a] Present address: Department of Physiology and Biophysics, Albert Einstein College of Medicine, Bronx, New York 10461.

[b] To whom all correspondence should be sent.

solidissima was not involved in the "shadow response" of the animal. Chalonzonitis *et al.* (1965) reported that giant hemoglobin-containing ganglion cells of *Aplysia deplians* decreased their firing rate when the hemoglobin was deoxygenated. Kraus and Colacino (1986) showed that under anoxic conditions nervous activity of *Tellina alternata* cerebro-visceral connectives with neurohemoglobin lasted about 20–30 minutes, slightly longer than the duration of neurohemoglobin deoxygenation, while nervous activity of *Tagelus plebeius* cerebro-visceral connectives without neurohemoglobin lasted only a few minutes after exposure to anoxic conditions.

The bivalve cerebro-visceral connective, as the major route for communication between the cerebropleural and the visceroparietal ganglia, is relatively long and easily extracted (Kraus *et al.*, 1988). It is a useful model for investigating tissue structure and function in relation to the neurohemoglobin-bound oxygen supply. Homologous cerebro-visceral connectives from *Tellina alternata* and *Spisula solidissima* with neurohemoglobin and *Tagelus plebeius* and *Geukensia demissa* without neurohemoglobin exhibit similar electrophysiological characteristics, which are generally dictated by axon size (0.3 μm diameter axons; Kraus *et al.*, 1988). Both types of connectives possess similar morphology but several ultrastructural characteristics of the neurohemoglobin-containing connectives reflect an anatomical design that may enhance the use of oxygen stored on the neurohemoglobin (Kraus *et al.*, 1988). In this paper we show how neurohemoglobin oxygen affinity characteristics were measured *in situ* under the constraints of cellular constituents and tissue geometry. Using this method, we can determine directly how neurohemoglobin operates *in situ* and begin to understand its utility within the organism.

Materials and Methods

Specimens of *Tellina alternata* and *Spisula solidissima* were collected and maintained as previously reported and cerebro-visceral connectives were dissected as described by Kraus *et al.* (1988).

Absorption spectra

Individual pieces (approximately 5 mm long) of freshly extracted cerebro-visceral connectives from *T. alternata* and *S. solidissima* were placed in the cylindrical sample chamber of a specially designed brass gas-slide (not between membranes; *cf.* Fig. 1, Colacino and Kraus, 1984). The 0.3 ml volume sample chamber, equipped with upper and lower lateral ports for control of gas tensions, was sealed with glass lids. The slide was also equipped with internal water coils for temperature control. Experiments were performed at 20 ± 0.5°C for *T. alternata* and 15 ± 0.5°C for *S. solidissima*. The slide was positioned in a single-beam microspectrophotometer constructed from monochromator, microscope, and photomultiplier (Colacino and Kraus, 1984). A 10 × 300 μm vertical light beam was passed through the center of the horizontal connective segment so that the pathlength of light was equal to the diameter of the connective. Voltage output from the photomultiplier was monitored and recorded by a computer-aided data logger.

Absorption spectra, recorded as the cerebro-visceral connectives were exposed to flowing humidified air, N_2 or CO, were obtained by collecting the intensities of light transmitted through the connective and through a blank (a region immediately adjacent to the connective) at 5 nm wavelength intervals from 500 to 600 nm. To avoid positional artifacts caused by moving the specimen in and out of the light path, all transmitted light intensities were taken consecutively, first through the specimen and then through the blank. Relative optical densities were calculated as the difference between the optical density at each wavelength and the optical density at 600 nm, the reference wavelength. (This wavelength was chosen as reference because absorption was minimal and changed little, compared to the peak absorption wavelengths, when the neurohemoglobin changed its derivative form; Colacino and Kraus, 1984.) This method produced consistent spectra by correcting for slow random electronic drift in transmitted light intensities through both sample and blank.

Heme concentration

Volume-averaged heme concentration was determined in whole cerebro-visceral connectives of *T. alternata* and *S. solidissima*. Individual connectives in seawater were placed between a glass slide and coverslip which were separated by glass microcapillaries. Connective diameters were measured with a calibrated ocular micrometer in the eyepiece of the microspectrophotometer. A 7 μm diameter light beam was shown through the center of the connectives. Absolute optical densities of the oxygenated connectives at two peak wavelengths (540 nm and 573 nm) were calculated from the intensities of light transmitted through the sample and through a blank. The absolute optical densities of cerebro-visceral connectives without neurohemoglobin (from *Tagelus plebeius* and *Geukensia demissa;* Kraus *et al.*, 1988) were then subtracted to cancel the absorption of cellular constituents other than neurohemoglobin.

Heme concentration was also determined in individual glial cells of *T. alternata*. Connective segments were placed in depression slides, cut longitudinally, and gently

teased to release the cells. Smooth spherical glial cells were easily distinguished from irregularly shaped neurons. Diameters of single glial cells were determined with the ocular micrometer. Absolute optical densities were obtained in the manner described for connective segments. Absorption due to cell membranes was assumed to be negligible.

Heme concentration was calculated with Beer-Lambert's law, using millimolar extinction coefficients for oxygenated *S. solidissima* neurohemoglobin (Strittmatter and Burch, 1963). Connective diameters or glial cell diameters were used as the light pathlength.

Molecular weight

Nearly entire nervous systems of seven *T. alternata* were carefully dissected, and portions of the nervous systems (cerebral and pedal ganglia and associated connectives) of approximately 150 *S. solidissima* were quickly excised and immersed in ice cold bivalve Ringer's (Willmer, 1978). The tissue samples were homogenized by hand in 2–3 ml cold 0.05 *M* KPO_4 buffer (pH 7.5) which contained 0.5 m*M* EDTA, and centrifuged at 10,000 × *g* for 20 min at 4°C. The pink supernatant was concentrated by N_2-pressurized ultrafiltration over an Amicon YM10 membrane (10,000 MW exclusion) at 4°C. Isolation and determination of apparent molecular sizes of the native neurohemoglobins were accomplished with fast protein liquid chromatography (FPLC, Pharmacia) using a 1 × 30 cm Superose 12 HR 10/30 column. The column was equilibrated with the same KPO_4 buffer at 30 ml/h flow rate and calibrated with 12,300–158,000 molecular weight protein standards at 20°C. The eluant was monitored at 280 nm. Absorption spectra of the collected fractions were obtained from 400 to 650 nm (Cary 17 spectrophotometer) to locate and isolate the neurohemoglobins.

Several samples of the isolated neurohemoglobins were run on denaturing sodium dodecyl sulfate (SDS) polyacrylamine gel electrophoresis (PAGE) and stained for protein with Coomassie Blue according to the methods described by Blackshear (1984). The series of protein standards (Pharmacia) ranged in molecular size from 14,400 to 94,000.

Oxygen and carbon monoxide equilibria

To measure the steady state oxygen affinity of neurohemoglobin *in situ*, short cerebro-visceral connective segments were placed in the gas-slide and arranged on the microspectrophotometer as described above. The input and output gas ports of the slide were connected to a closed circuit gas delivery system. The system consisted of a 4.6 liter glass gas mixing reservoir fitted with a polarographic oxygen sensor (with sensitivity of 0.1 mm Hg; Beckman 742 Oxygen Analyzer) and a reciprocating pump with ceramic cylinder and carbon piston (FMI). The system components were connected with 18 gauge stainless steel tubing (Small Parts, Inc.) and short couplings of thick-walled Tygon capillary tubing (Cole-Palmer). The gas reservoir was immersed in a temperature-controlled water bath. The bath also provided coolant flow to the gas-slide. All gases were humidied and the rate of gas flow through the circuit was approximately 100 ml/min.

Neurohemoglobin fractional saturation at different oxygen tensions was measured as follows. A single connective segment in the gas-slide sample chamber was exposed to flowing humidified room air. Gas flow occurred through lateral ports both above and below the specimen, thus ensuring rapid and total exposure of the specimen to the gas. An oxygenated neurohemoglobin spectrum was recorded. The slide was then flushed with humidified 99.999% N_2 to deoxygenate the neurohemoglobin. Transmitted light intensity at 560 nm, continuously monitored by the photomultiplier, was recorded with an X-Y recorder (Heathkit IR-5207). A deoxygenated neurohemoglobin spectrum was recorded when the light intensity reached an asymptote, usually in less than one hour. The neurohemoglobin was then reoxygenated in steps of 0.2–0.4 mm Hg PO_2, with absorption spectra recorded after equilibration at each PO_2. Fractional saturation was calculated from optical densities at two wavelength pairs (575 and 560 nm, 560 and 540 nm; Rossi-Fanelli and Antonini, 1958). The partial pressures of oxygen at half saturation (P_{50}) and apparent cooperativity (Hill number) for oxygen binding *in situ* were calculated from the Hill equation.

Carbon monoxide affinities of oxyneurohemoglobin and deoxyneurohemoglobin *in situ* were determined in a similar manner, except that the connectives were first exposed to air or N_2, respectively, and then to stepwise increases in PCO.

Oxygen unloading kinetics

The oxygen unloading kinetics of the neurohemoglobin *in situ* were determined with the previously described microspectrophotometer arrangement. The gas-slide containing a segment of cerebro-visceral connective was first flushed with humidified room air and an oxyneurohemoglobin spectrum was recorded. The sample chamber was then flushed with humidified 99.999% N_2 and changes in light intensity at 560 nm were recorded with the X-Y recorder. The calculated time for a cylindrical air-equilibrated 0.3 ml volume sample chamber to reach 0.01 mm Hg PO_2 is approximately 2.5 s (assuming a well-mixed

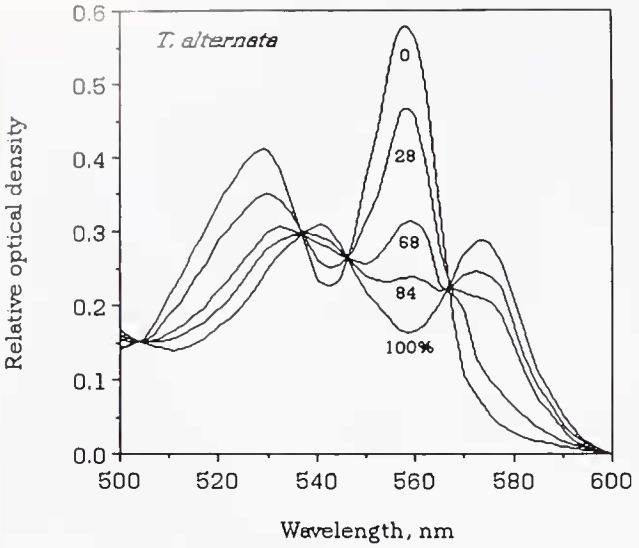

Figure 1. The oxygen equilibrium spectrogram of *Tellina alternata* cerebro-visceral connective neurohemoglobin *in situ* from 0% oxyneurohemoglobin (deoxyneurohemoglobin) to 100% oxyneurohemoglobin. Intermediate spectra were taken at 0.85, 1.55, and 2.01 mm Hg PO_2. The unusual deoxyneurohemoglobin spectrum exhibits two wavelength maxima. The spectrogram of *Spisula solidissima* neurohemoglobin *in situ*, collected at higher PO_2, is identical.

chamber), which is well below the time required for neurohemoglobin deoxygenation, approximately 30 min. At 3–5 min intervals, transmitted light intensities at 600, 575, 560, and 540 nm were recorded. A deoxyneurohemoglobin spectrum was recorded when the light intensity trace reached an asymptote. Humidified air was then reintroduced to the sample chamber and the change in light intensity at 560 nm during reoxygenation of the neurohemoglobin was recorded. Neurohemoglobin fractional saturation, calculated as before, was plotted as a function of time. The oxygen unloading rate *in situ* was calculated as the product of the slope of this curve and the heme concentration.

Oxygen dissociation using humidified CO as the deoxygenating gas was measured in a similar manner. Light intensities were collected at 570 and 535 nm, the peak wavelengths for carbon monoxide hemoglobin. In several experiments, a few crystals of dithionite were added to the seawater surrounding connective segments in a depression slide. The well was quickly sealed with a cover slip and absorption spectra were collected immediately thereafter.

Results

Spectral characteristics, heme concentration, and molecular weight

The oxyneurohemoglobin spectrum (see Fig. 1) and carbon monoxide neurohemoglobin spectrum (not shown) of *T. alternata* and *S. solidissima* cerebro-visceral connectives are similar to those of other hemoglobins. However, a distinguishing feature is the deoxyneurohemoglobin spectrum which exhibits two clear absorption maxima near 558 and 529 nm (see Fig. 1; deoxyhemoglobin typically exhibits a single maximum at approximately 555 nm). Although this spectrum is unusual, it is not unique and has been previously reported for the extracted neurohemoglobin of *S. solidissima* (Strittmatter and Burch, 1963) and the circulating plasma in the choroid rete mirabile of two fish, *Amia calva* and the bluefish (Wittenberg and Wittenberg, 1975).

The volume-averaged heme concentrations and cerebro-visceral connective diameters of *T. alternata* and *S. solidissima* are presented in Table I. Neurohemoglobin was detected spectrophotometrically only in glial cells teased from connectives and ganglia, not in ganglion cells. The heme concentration of individual *T. alternata* glial cells is 5.9 ± 1.3 m*M* (average diameter 21.2 ± 2.7 μm; n = 12), which is approximately twice the concentration in whole connectives (Table I). In accordance, glial cells represent roughly one half the cerebro-visceral connective volume because about 44% of the volume consists of axons (Kraus *et al.*, 1988), and extracellular volume is estimated at about 10% in nervous tissue (Willmer, 1978).

On the FPLC, the neurohemoglobins eluted as single dominant peaks at 28.9 ± 0.2 min (n = 3) and 29.0 ± 0.2 min (n = 3), corresponding to molecular sizes of 33,200 ± 1900 for *T. alternata* and 31,800 ± 2700 for *S. solidissima*, respectively. Elution times of neurohemoglobins and protein standards are presented in Figure 2. On denaturing gel electrophoreses, single wide bands were lo-

Table I

Characteristics of Tellina alternata *and* Spisula solidissima *cerebro-visceral connectives and neurohemoglobin* in situ

Parameter	*Tellina alternata*	*Spisula solidissima*
Connective diameter (μm)	126 ± 22 (8)*	184 ± 35 (15)
Heme concentration (m*M*)	3.05 ± 0.26 (18)	1.50 ± 0.25 (24)
O_2 P_{50} (mm Hg)	1.3 ± 0.4 (16)	2.3 ± 0.3 (12)
O_2 Hill number	3.7 ± 0.9 (16)	2.1 ± 0.4 (12)
CO P_{50} in air (mm Hg)	0.5 ± 0.2 (8)	1.3 ± 0.6 (4)
CO Hill number in air	2.0 ± 0.3 (8)	3.0 ± 1.2 (4)
CO P_{50} in N_2 (mm Hg)	0.06 ± 0.01 (9)	0.4 ± 0.2 (4)
CO Hill number in N_2	3.0 ± 1.0 (9)	4.1 ± 1.2 (4)
Linear unloading rate with N_2 (nmol O_2 g^{-1} min^{-1})	146.2 ± 37.9 (12)	100.2 ± 24.3 (12)

* Numbers are given as average ± standard deviation (number of repetitions).

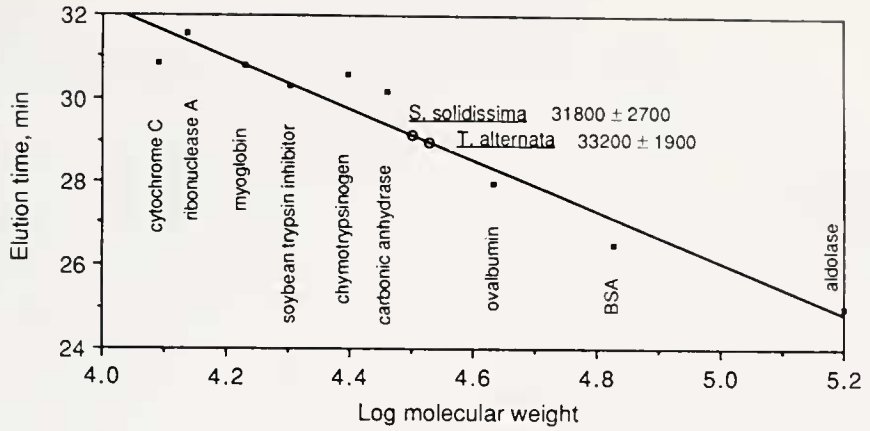

Figure 2. Molecular size determination of bivalve neurohemoglobins compared to protein standards on a Superose 12 HR 10/30 column using fast protein liquid chromatography.

cated at positions corresponding to approximately 15,000 for both neurohemoglobins, about one half the size of the native proteins. The apparent molecular sizes of both neurohemoglobins are quite similar, and each putative dimer may be composed of a single type of monomer. In general, molluscan intracellular hemoglobins in organs such as muscles, gills, and nerves are monomers or dimers with one heme per 15,000–17,000 daltons (Terwilliger and Terwilliger, 1985). Earlier reports estimated the molecular size of *S. solidissima* neurohemoglobin to be 20,000 using sedimentation coefficients (Strittmatter and Burch, 1963).

Oxygen and carbon monoxide equilibria

Characteristic absorption spectra during stepwise neurohemoglobin oxygenation are shown in Figure 1. Representative saturation curves are shown in Figure 3. Both neurohemoglobins have high oxygen affinities and exhibit high Hill numbers *in situ* (Table I). Carbon monoxide affinities of both oxygenated neurohemoglobins are in agreement with several other invertebrate hemoglobins (Table I; Wittenberg *et al.*, 1965; Bonaventura and Bonaventura, 1983). Both neurohemoglobins have a much higher affinity for CO in the absence of oxygen (Table I).

Oxygen unloading kinetics

The neurohemoglobins of *T. alternata* and *S. solidissima* required approximately 30 and 20 min, respectively, to reach 98% deoxygenation when exposed *in situ* to high purity N_2 (Fig. 4). Under these conditions, deoxygenation proceeded in a mostly linear manner that lasted approximately 70% and 50% of the total unloading duration for *T. alternata* and *S. solidissima*, respectively. The linear oxygen unloading rates are listed in Table I. In contrast, both neurohemoglobins required less than three minutes to deoxygenate when exposed *in situ* to CO. Moreover, connective segments exposed to dithionite deoxygenated in less than 2 min, the time required to place the slide on the microspectrophotometer. Dithionite creates an anoxic environment by chemically scavenging any dissolved oxygen. When fully deoxygenated and then exposed to air *in situ*, both neurohemoglobins required approximately 5 s to become fully reoxygenated.

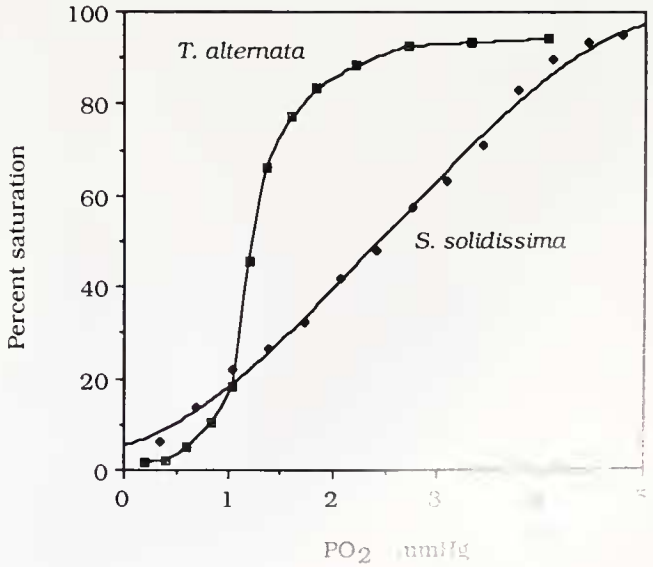

Figure 3. Steady state oxygen saturation of cerebro-visceral connective neurohemoglobins *in situ* as a function of PO_2. Both neurohemoglobins exhibit a small PO_2 range for loading and unloading, although the range for *Tellina alternata* neurohemoglobin is more narrow than the range for *Spisula solidissima* neurohemoglobin.

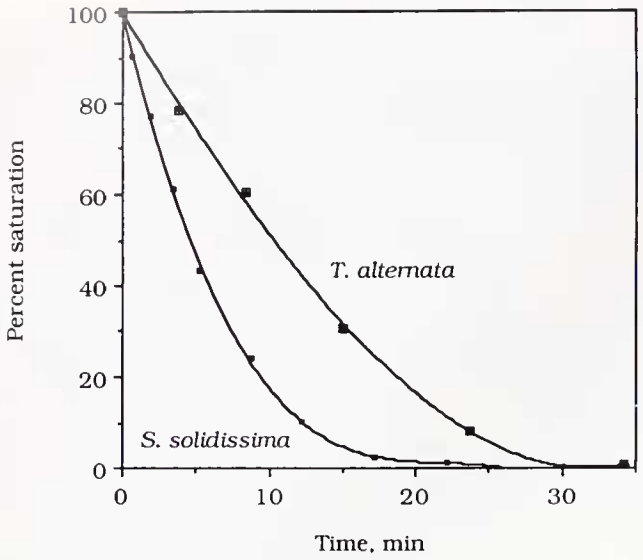

Figure 4. The change in saturation of cerebro-visceral connective neurohemoglobins *in situ* as a function of time after the start of anoxic conditions. Both curves display long duration and are linear throughout a large portion of the process.

Discussion

The red pigment in the nervous systems of *T. alternata* and *S. solidissima* is hemoglobin as evidenced by its reversible oxygenation and characteristic oxyhemoglobin and carbon monoxide hemoglobin absorption spectra. The unusual deoxyneurohemoglobin spectrum—known to be produced by pyridine hemochromagen—suggests that both the proximal and distal ligand positions of the ferrous heme iron may be ligated to nitrogenous or sulfurous groups when deoxygenated (Wittenberg and Wittenberg, 1975). This molecular arrangement may be due to reversible changes in configuration that allow intrinsic or extrinsic amino acid groups to compete for the heme distal ligand position or it may be due to partial denaturation of the protein (Wittenberg and Wittenberg, 1975). Because repeated conversion from oxyneurohemoglobin to deoxyneurohemoglobin showed no spectral signs of pigment denaturation or decrease in concentration, the hemochromagen spectrum was accepted as normal for this neurohemoglobin.

The heme concentration of both *T. alternata* and *S. solidissima* cerebro-visceral connectives is high compared to other hemoglobin-containing nerves. The heme concentration in *Aplysia depilans* ganglia, determined by a method similar to ours, was 0.04–0.1 m*M* (Chalonzonitis *et al.*, 1965). Here, the neurohemoglobin is located within giant ganglion cells and not in the glia (Chalonzonitis *et al.*, 1965). The heme concentration in the nerves of *Aplysia californica* and *Aphrodita aculeata*, determined by extraction procedures, was 0.1 and 0.7 m*M*, respectively (Wittenberg *et al.*, 1965). Neurohemoglobin concentration influences the magnitude and duration of the oxygen supply to the connectives (see below).

To understand the role of neurohemoglobin in the supply of oxygen to the axons of the cerebro-visceral connective, we consider three features of the system: (1) the geometric location of the neurohemoglobin in relation to the exterior of the connective and the oxygen-consuming axons; (2) the steady state oxygen affinity of the neurohemoglobin; and (3) the unloading kinetics of the neurohemoglobin-bound oxygen supply. In each case, the oxygen supply system of the cerebro-visceral connective of *T. alternata* operates within more restricted conditions, but the systems of both *T. alternata* and *S. solidissima* behave in a similar manner.

The bivalve cerebro-visceral connective consists of a cylindrical core of oxygen-consuming glial cells and axons, and a thin outer sheath of acellular, non-oxygen-consuming material (Kraus *et al.*, 1988). Axons transmit nervous information, glial cells offer physiological support to the axons, and the sheath provides structural support for the core. Neurohemoglobin-containing glial cells ramify extensively throughout the core to ensheath bundles of axons (Kraus *et al.*, 1988), resulting in a nearly uniform mixture of axons and entwining glial cells. Because both neurohemoglobins possess relatively low P_{50}s and high Hill numbers *in situ* (Table I) and the connectives exhibit a moderate oxygen consumption rate during activity (Kraus and Doeller, submitted), an oxyhemoglobin gradient necessary for facilitated diffusion would occur only if the connectives were exposed to a narrow and low range of ambient PO_2. The anterior portion of the cerebro-visceral connective is buried deep within the foot muscle while the posterior portion is located beneath the siphons. In addition, siphonal nerves possess neurohemoglobin with identical oxygen binding characteristics *in situ* as the connective neurohemoglobin (unpub. data), and are directly exposed to siphonal currents. Therefore, the proper PO_2 regime for facilitated diffusion from mantle fluid or from hemolymph to axons may exist at specific locations or at specific times.

Both neurohemoglobins exhibit high oxygen affinities (Table I). *T. alternata* neurohemoglobin is 95% saturated at about 3 mm Hg PO_2, computed from the Hill equation. Thus, oxygen delivery begins at a PO_2 slightly higher than 3 mm Hg. Likewise, *S. solidissima* neurohemoglobin begins to deliver oxygen at a PO_2 slightly higher than 6 mm Hg. In addition, both neurohemoglobins exhibit substantial apparent cooperativity *in situ* (Table I) and load and unload oxygen over a narrow range of PO_2 near the P_{50} of each neurohemoglobin (Fig. 3).

Neurohemoglobin could function as an oxygen store for the cerebro-visceral connective if it began to release oxygen near the PO_2 at which simple diffusion into the connective began to limit the oxygen consumption rate. This diffusion-limiting PO_2 can be calculated using the diffusion equations for a cylindrical shell (sheath) and a cylindrical core (connective) (from Hill, 1928):

$$PO_2 = [nO_2(r_o^2 - r_i^2)/(4D_c)] + [(nO_2 r_i^2)/(4D_n)]$$

where PO_2 is the external partial pressure of oxygen (atm) (assuming zero PO_2 at the center of the core), nO_2 is the specific oxygen consumption rate of the connective (nmol O_2 g^{-1} min^{-1}), r_i is the core radius (cm), r_o is the total radius (cm), and D_n and D_c are Krogh's diffusion coefficients for oxygen in muscle tissue [used here for nervous tissue, following the example of Hill (1928)] and collagen, respectively (converted to nmol O_2 cm^{-2} min^{-1} $(atm/cm)^{-1}$). For *T. alternata* cerebro-visceral connective, nO_2 is approximately 101.4 nmol O_2 g^{-1} min^{-1} during activity (Kraus and Doeller, submitted), r_i is 0.00609 cm, r_o is 0.0063 cm, and D_n is 5.98×10^{-1} and D_c is 4.91×10^{-1} nmol O_2 cm^{-2} min^{-1} $(atm/cm)^{-1}$ (Krogh, 1941). (We assume that the oxygen-consuming centers are evenly distributed throughout the connective core.) The calculated diffusion-limiting PO_2 for *T. alternata* cerebro-visceral connective is 1.3 mm Hg (1.2 mm Hg for the connective core and an additional 0.1 mm Hg for the sheath). For *S. solidissima* cerebro-visceral connective, nO_2 is approximately 96.2 nmol O_2 g^{-1} min^{-1} during activity (Kraus and Doeller, submitted), r_i is 0.0092 cm, and r_o is 0.0089 cm. The calculated diffusion-limiting PO_2 for *S. solidissima* cerebro-visceral connective is 2.8 mm Hg (2.6 mm Hg for the core and an additional 0.2 mm Hg for the sheath).

The calculated diffusion-limiting PO_2 for each connective is lower than the PO_2 at which each neurohemoglobin begins to unload oxygen (see above). If this were true *in vivo*, the diffusion rate of oxygen would not become limiting until 40–50% of the neurohemoglobin was deoxygenated. In this case, any oxygen released before diffusion-limiting conditions were reached would probably diffuse towards the oxygen-consuming axons, but would be superfluous because simple diffusion of dissolved oxygen could also supply the axons. However, if the perineural sheath was a more effective barrier to oxygen diffusion by possessing a lower diffusion coefficient than collagen or if other adjacent tissues or unstirred layers acted as additional diffusion boundaries, the diffusion-limiting PO_2 would be closer to the initial unloading PO_2 and the neurohemoglobin would be a more useful oxygen store.

The perineural sheath of both neurohemoglobin-containing cerebro-visceral connectives consists of many concentric layers of electron-dense material (*cf.* Fig. 2, Kraus *et al.*, 1988). This ultrastructure, which is unlike the ultrastructure of the more typical perineural sheath of neurohemoglobinless cerebro-visceral connectives (Kraus *et al.*, 1988), may reduce the sheath's oxygen permeability. Although a less permeable sheath would resist oxygen diffusion, the PO_2 within the tissues would probably be high enough under normoxic conditions (37–111 mm Hg, Booth and Mangum, 1978) that oxygen diffusion *into* the connective would be virtually unimpeded. However, under anoxic conditions or oxygen tensions low enough to deoxygenate the neurohemoglobin, oxygen diffusion *out of* the connective could be substantially reduced. In fact, an important function of this perineural sheath may well be to retain oxygen within the connective during anoxic conditions. Experiments are underway to determine the biochemical composition of the perineural sheaths from connectives with and without neurohemoglobin.

Two important features of the oxygen unloading reaction *in situ* are the long duration and the linearity throughout most of the unloading process (Fig. 4). Few studies have investigated the duration of tissue hemoglobin oxygen unloading *in situ* or *in vivo* where unloading behavior can be modified by cellular constituents and body geometry. The hemoglobin located in the lateral nerve cords of the nemertine *Amphiporus lactifloreus* deoxygenated in about 3 min when the animal was sealed between a glass slide and cover slip and denied access to oxygen (Varndell, 1980). In contrast, the hemoglobin of the microscopic vermiform gastrotrich *Neodasys* spp. (less than 50 μm in diameter) required nearly one hour to deoxygenate when the animal was placed between two 6 μm Teflon membranes and exposed to 99.999% N_2 (Colacino and Kraus, 1984). Similarly, the hemoglobin in the anterior hypodermal cells of the nematode *Mermis nigrescens* remained oxygenated for more than two hours when perfused with Ringer's solution equilibrated with high purity N_2 (Burr and Harosi, 1985).

In general, oxygen unloading from a hemoglobin-containing tissue can be limited either by the molecular dissociation rate of the hemoglobin (unloading is reaction-limited) or by the diffusion rate out of the tissue (unloading is diffusion-limited) (Colacino *et al.*, 1987). An oxygen molecule once dissociated can be removed from the tissue via metabolic consumption or diffusion to the exterior, or it can reassociate on [illegible] to other deoxyhemoglobin molecules. Once the oxygen molecule reaches the tissue exterior, it can be removed from the boundary layer by diffusion or convection. With little or no diffusion resistance within or surrounding the tissue, unloading time will be controlled by the molecular dissociation rate. In this case, long unloading

times will be displayed by hemoglobins with low dissociation rate constants. For example, the hemoglobin of *Ascaris lumbricoides* would require more than 15 min to deoxygenate, given its rate constant (0.004 s^{-1}) determined by stopped-flow techniques (Gibson and Smith, 1965).

The possibility that neurohemoglobin may possess low molecular dissociation rates was investigated by using CO or dithionite to deoxygenate the neurohemoglobin. Because neurohemoglobin exhibits a much higher affinity for CO than oxygen (Table I), CO preferentially binds to any heme iron exposed by oxygen dissociation. Oxygen reassociation is thus prevented and the rate of oxygen dissociation *in situ* can be approached, limited mostly by the rate of CO diffusion into the connective. Under these conditions, deoxygenation times were greatly reduced (see Fig. 5A, curve c). Dithionite, which scavenges oxygen, also greatly reduced deoxygenation times. The neurohemoglobin, therefore, probably does not have an exceptionally low molecular dissociation rate, and oxygen unloading from the connective is not reaction-limited.

The unloading time of a diffusion-limited reaction is controlled by the combined effect of the diffusion rate of oxygen out of the region plus the number of dissociations and reassociations that take place before oxygen reaches the exterior (Colacino *et al.*, 1987). The diffusion rate can be limited by a specific diffusion boundary located between the hemoglobin and the exterior. Moreover, the reassociation of oxygen to deoxyhemoglobin is more likely when hemoglobin concentration is high and when oxygen permeability of the diffusion boundary is low. These factors will lengthen oxygen unloading times. Preliminary data indicate that unloading times are shorter when neurohemoglobin concentration is effectively lowered by partial inactivation with CO.

The time for oxygen unloading can be estimated from the quantity of neurohemoglobin-bound oxygen and the diffusion rate across the sheath, assuming the sheath represents the principle diffusion barrier. The steady state rate of diffusion (neglecting metabolism) out of a 1 cm length of cylindrical shell like a sheath, Q (nmol O_2 cm^{-1} min^{-1}), can be calculated using

$$Q = (2\pi D_c dPO_2)/\ln (r_o/r_i)$$

where D_c is Krogh's diffusion coefficient for oxygen in collagen (4.91×10^{-1} nmol O_2 cm^{-2} min^{-1} $(atm/cm)^{-1}$), dPO_2 is the partial pressure difference across the sheath (atm), and r_o and r_i are the outside and inside radii (cm), respectively, of the cylinder (Jacobs, 1967). This steady state equation was selected because the neurohemoglobin unloading rate is nearly constant throughout most of its duration, although more so in *T. alternata* than in

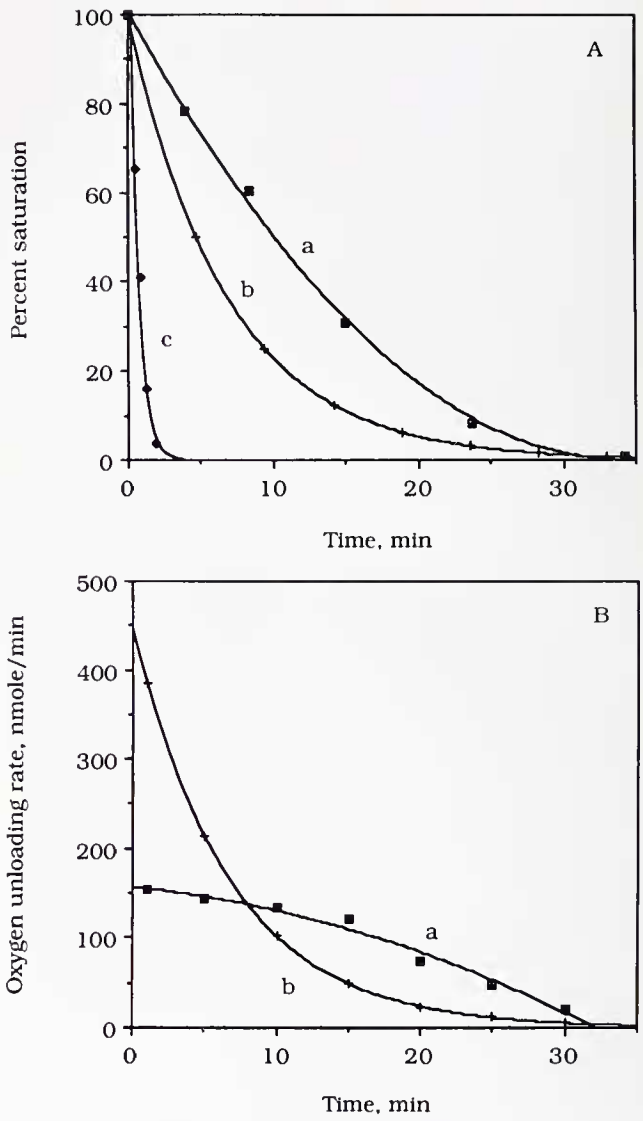

Figure 5. A. (a) The oxygen unloading curve of *Tellina alternata* cerebro-visceral connective neurohemoglobin *in situ*. (b) A hypothetical exponential unloading curve of the same duration as curve a. (c) The oxygen unloading curve of *Tellina alternata* neurohemoglobin *in situ* with CO as the deoxygenating gas. B. (a) The derivative of curve a in A. (b) The derivative of curve b in A. (See text for discussion.)

S. solidissima (Fig. 4). A nearly constant unloading rate implies that neither the partial pressure gradient nor the diffusion distance is changing within the core of the connective, thus we assume that the core is a well-mixed solution at constant PO_2 near the P_{50} (see below; Honig *et al.*, 1986). For an average *T. alternata* connective, dPO_2 is 1.3 mm Hg (Table I) or 1.71×10^{-3} atm, and r_o and r_i are defined previously. The calculated steady state rate of diffusion, Q, is 1.6×10^{-1} nmol O_2 min^{-1} cm^{-1}. The quantity of oxygen in this 1 cm segment is 3.8×10^{-1}

nmol O_2, computed from the cylinder volume and the average heme concentration (Table I). Dissolved oxygen is negligible at this low PO_2. The unloading time, computed by dividing the quantity of oxygen by the rate Q, is 2.4 min. The unloading time computed for an average *S. solidissima* connective segment is 1.4 min, using 4.0×10^{-1} nmol O_2 per 1 cm segment and 2.3 mm Hg dPO_2 to give a Q of 2.8×10^{-1} nmol O_2 min^{-1} cm^{-1}. Both calculated times are clearly shorter than the observed 20 min and 10 min, respectively, for the approximate linear portion of the unloading process (Fig. 4), but again, they would be longer if the oxygen permeability of the sheath were lower or if dPO_2 was smaller.

The second unusual feature of the oxygen unloading reaction *in situ* is its linearity during a large portion of the process. The apparently cooperative nature of neurohemoglobin *in situ* may be responsible for this phenomenon. Because PO_2 in the connective is effectively held within a narrow range near the P_{50} (Fig. 3), the driving force for unloading is nearly constant. In this study both native neurohemoglobins have been isolated only as oxygenated dimers, but further subunit interaction is possible. Cooperativity results from subunit interaction which for some hemoglobins is enhanced by aggregation upon deoxygenation (Chiancone *et al.*, 1981; Tam and Riggs, 1984; Wells *et al.*, 1984).

To illustrate the physiological significance of the unusual oxygen unloading features (Fig. 5A), the neurohemoglobin dissociation reaction *in situ* (curve a) and an hypothetical first order dissociation reaction (curve b) of equal duration are presented for comparative purposes. The derivatives of both reactions plotted against time (Fig. 5B) indicate how changes in the oxygen unloading rate with time differ between the two types of reactions. The neurohemoglobin unloading rate (Fig. 5B, curve a) is nearly constant and independent of oxyhemoglobin concentration throughout most of the unloading process. In contrast, the unloading rate of the exponential reaction (Fig. 5B, curve b) is proportional to oxyhemoglobin concentration and thus declines with time.

We argue that the geometric design of the neurohemoglobin-containing cerebro-visceral connective and the oxygen affinity characteristics of the neurohemoglobin are concurrently responsible for the magnitude and duration of the neurohemoglobin-released oxygen supply. An oxygen supply at a constant rate for an extended period of time would clearly be useful to an animal requiring aerobic nervous function during anoxic conditions, and both *T. alternata* and *S. solidissima* often burrow into anoxic muds. In a subsequent paper, we investigate the system's efficiency, including the amount of neurohemoglobin-released oxygen actually consumed by the connective and how well the connective maintains activity under anoxic conditions (Kraus and Doeller, submitted).

Acknowledgments

Portions of this paper represent part of a Ph.D. dissertation submitted by D.W.K. to Clemson University. We thank Dr. James M. Colacino for guidance and discussion during this research, Mr. T. L. Vandergon for helpful discussion, and Drs. J. B. and B. A. Wittenberg for useful instruction. This work was supported in part by grants from the Lerner-Grey Fund for Marine Research, the Slocum-Lunz Foundation, and Sigma Xi.

Literature Cited

Blackshear, P. J. 1984. Systems for polyacrylamide gel electrophoresis. Pp. 237–255 in *Methods of Enzymology* **104,** W. B. Jakoby, ed. Academic Press, New York.

Bonaventura, C., and J. Bonaventura. 1983. Respiratory pigments: Structure and function. Pp. 1–50 in *The Mollusca, Vol. 2,* K. M. Wilber, ed. Academic Press, New York.

Booth, C. E., and C. P. Mangum. 1978. Oxygen uptake and transport in the lamellibranch mollusc *Modiolus demissus*. *Physiol. Zool.* **51:** 17–32.

Burr, A. H., and F. I. Harosi. 1985. Naturally crystalline hemoglobin of the nematode *Mermis nigrescens*. An *in situ* microspectrophotometer study of chemical properties and dichroism. *Biophys. J.* **47:** 527–536.

Chalazonitis, N., M. Gola, and A. Arvanitaki. 1965. Microspectrophotométrie différentielle sur des neurones géants in vivo (*Aplysia depilans*). Mesure de la diffusibilité de l'oxygène. *C. R. Soc. Biol.* **159:** 2240–2245.

Chiancone, E., P. Vecchini, D. Verzili, F. Ascoli, and E. Antonini. 1981. Dimeric and tetrameric hemoglobins from the mollusc *Scapharca inaequivalvis*. *J. Mol. Biol.* **152:** 577–592.

Colacino, J. M., and D. W. Kraus. 1984. Hemoglobin-containing cells of *Neodasys* (Gastrotricha, Chaetonotida). II. Respiratory significance. *Comp. Biochem. Physiol.* **79A:** 363–369.

Colacino, J. M., J. R. Brannan, and M. Fields. 1987. A model for oxygen storage by hemoglobin. *J. Theor. Biol.* **126:** 437–447.

Gibson, Q. H., and M. H. Smith. 1965. Rates of reaction of *Ascaris* hemoglobins with ligands. *Proc. R. Soc. Lond. B* **163:** 206–214.

Heatwole, D. W. 1981. Spawning and respiratory adaptations of the ophiuroid, *Hemipholis elongata* (Say) (Echinodermata). Masters Thesis, University of South Carolina.

Hill, A. V. 1928. The diffusion of oxygen and lactic acid through tissues. *R. Soc. Proc. B* **104:** 39–96.

Honig, C. R., T. E. J. Gayeski, W. Federspiel, A. Clark Jr., and P. Clark. 1984. Muscle O_2 gradients from hemoglobin to cytochrome: new concepts, new complexities. In *Oxygen Transport to Tissue V*, D. W. Lubbers, H. Acker, E. Leniger-Follert, and T. [illegible] eds. *Adv. Exp. Med. Biol.* **169:** 23–38.

Jacobs, M. H. 1967. *Diffusion Processes.* Springer, [illegible]

Kennedy, D. 1960. Neural photoreception in a lamellibranch [illegible] *J. Gen. Physiol.* **44:** 277–299.

Kraus, D. W., and J. M. Colacino. 1984. The oxygen consumption rates of three gastrotrichs. *Comp. Biochem. Physiol.* **79A:** 691–693.

Kraus, D. W., and J. M. Colacino. 1986. Extended oxygen delivery from the nerve hemoglobin of *Tellina alternata* (Bivalvia). *Science* **232:** 90–92.

Kraus, D. W., J. E. Doeller, and P. R. Smith. 1988. A physiological comparison of bivalve mollusc cerebro-visceral connectives with and without neurohemoglobin. I. Ultrastructural and electrophysiological characteristics. *Biol. Bull.* **174:** 54–66.

Krogh, A. 1941. *The Comparative Physiology of Respiratory Mechanisms.* University of Pennsylvania Press, Philadelphia. 172 pp.

Mangum, C. P., B. R. Wooden, C. Bonaventura, B. Sullivan, and J. Bonaventura. 1975. The role of coelomic and vascular hemoglobin in the annelid family Terrebelidae. *Comp. Biochem. Physiol.* **51A:** 281–294.

Rossi-Fanelli, A., and E. Antonini. 1958. Studies on the oxygen and carbon monoxide equilibria of human hemoglobin. *Arch. Biochem. Biophys.* **77:** 478–492.

Strittmatter, P., and H. B. Burch. 1963. The hemeprotein in ganglia of *Spisula solidissima*. *Biochim. Biophys. Acta* **78:** 562–563.

Tam, L-T., and A. F. Riggs. 1984. Oxygen binding and aggregation of bullfrog hemoglobin. *J. Biol. Chem.* **259:** 2610–2616.

Terwilliger, R. C., and N. B. Terwilliger. 1985. Molluscan hemoglobins. *Comp. Biochem. Physiol.* **81B:** 255–261.

Varndell, I. M. 1980. Oxygen consumption and the occurrence of a haemoprotein within the central nervous tissue of the hoplonemertean *Amphiporus lactifloreus* (Johnson) (Nemertea: Enopla: Monostilifera). *J. Exp. Mar. Biol. Ecol.* **45:** 157–172.

Wells, R. M. G., M. J. Hudson, and T. Brittain. 1981. Function of the hemoglobin and the gas bubble in the backswimmer *Anisops assimilis* (Hemiptera: Notonectidae). *J. Comp. Physiol. B* **142:** 515–522.

Willmer, P. G. 1978. Volume regulation and solute balance in the nervous tissue of an osmoconforming bivalve (*Mytilus edulis*). *J. Exp. Biol.* **77:** 157–179.

Wittenberg, J. B., and B. A. Wittenberg. 1975. A hemeprotein implicated in oxygen transport into the eye of fish. *Comp. Biochem. Physiol.* **51A:** 425–429.

Wittenberg, B. A., R. W. Briehl, and J. B. Wittenberg. 1965. Haemoglobins of invertebrate tissues. Nerve haemoglobins of *Aphrodita*, *Aplysia*, and *Halosydna*. *Biochem. J.* **96:** 363–371.